

Effect of Stacking Sequence on the Temperature Distribution in a Composite Multi-ply Laminates Vessel

M. Shariati, M.H. Keyhani and I. Shalchian

Department of Mechanical Engineering, Shahrood University of Technology, Shahrood, Iran

Abstract: Due to high solidity to weight ratio of composite they have been used widely. A many all the special features of composites, the layers arrangement, heat transfer and convection in these kinds of materials are of the most important features of them. Since heat conductivity of composite are dependent on the direction, they are grouped both in isotropic and anisotropic material and thermal analysis of them is possible no matter of symmetrical or non-symmetrical boundary condition, they have important rate in scientific and engineering courses.

Key words: Heat transfer . stacking sequence . temperature distribution . composite pressure vessel

INTRODUCTION

At recent years, many researches are carried out about different solutions methods on the heat transfer of anisotropic materials. Generally, in a lot of engineering problems, it is necessary to know heat flow and thermal distribution in multi-layers composites.

Many of researchers have been tried to solve the heat transfer problems (conduction and radiation and so on) in the composite materials. For example, Bularvin and Kashchov [1] and Mulholland and Cobble [2] have been solved heat transfer on the anisotropic multi-layers composite materials.

A general solution methods including of experimental heat transfer tests in composite materials are carried out by Han and Cosner [3], Azcvedeo *et al.* [4], Chen *et al.* [5], Archer and Horne, Takao and Taya [6], Okey [7], Miller and Weaver [8], Tittle and Robinson [9], DeMonte [10], Onyejekwe [11], Heisler [12] and Ozisik [13].

In this paper, Energy equation and heat flow is studied for anisotropic solids and heat conduction tensor is obtained for this materials. Then, the tensor components are obtained for a composite laminate.

The analytical solution of such problems is not possible, because of their difficulties. Thus, the numerical solution is used.

ANALYTICAL FORMULATIONS

Generally, the flux relations for orthogonal curvilinear coordinate system (u_1, u_2, u_3) can be expressed as:

$$q_i = - \sum_{j=1}^3 \frac{1}{a_j} k_{ij} \frac{\partial T}{\partial u_j} \quad i = 1, 2, 3 \quad (1)$$

The energy equation in orthogonal curvilinear coordinate system (u_1, u_2, u_3) for anisotropic solids is:

$$\frac{1}{a_1 a_2 a_3} \left[\begin{array}{c} \frac{\partial}{\partial u_1} (a_2 a_3 q_1) + \\ \frac{\partial}{\partial u_2} (a_1 a_3 q_2) + \\ \frac{\partial}{\partial u_3} (a_1 a_2 q_3) \end{array} \right] - g = -\rho C_p \frac{\partial T}{\partial t} \quad (2)$$

Where a_j is transformation factor. Cylindrical coordinates (r, ϕ, z):

$$u_1 = r \quad a_1 = 1$$

$$u_2 = \phi \quad a_2 = r$$

The nine heat conductivity coefficients of k_{ij} matrix, are the components of a second order tensor. In the triclinic system, the symmetrical or non-symmetrical conditions does not change the number of conductivity coefficients; so all the nine k_{ij} coefficients can be non-zero [14].

$$\bar{k} = \begin{bmatrix} k_{11} & k_{12} & k_{13} \\ k_{21} & k_{22} & k_{23} \\ k_{31} & k_{32} & k_{33} \end{bmatrix} \quad (3)$$

Due to symmetric planes in this problem, the conductivity tensor reduces to [15]:

$$\bar{k} = \begin{bmatrix} k_{11} & 0 & 0 \\ 0 & k_{22} & 0 \\ 0 & 0 & k_{22} \end{bmatrix} \quad (4)$$

If the direction of coordinate system axes to be not parallel with the fiber direction, using the transformation tensor, we can determine the heat transfer coefficients on the desired axis directions.

The off-axis conductivity matrix components can be expressed as [16]:

$$[\bar{k}] = \begin{bmatrix} k_{11} \sin^2 \theta + k_{22} \cos^2 \theta & (k_{11} - k_{22}) \sin \theta \cos \theta & 0 \\ (k_{11} - k_{22}) \sin \theta \cos \theta & k_{11} \cos^2 \theta + k_{22} \sin^2 \theta & 0 \\ 0 & 0 & k_{22} \end{bmatrix} \quad (5)$$

The energy equation of a laminate is represented as follow:

$$\begin{aligned} & (k_{11} \cos^2 \theta + k_{22} \sin^2 \theta) \frac{1}{r} \frac{\partial}{\partial r} \left(r \frac{\partial T}{\partial r} \right) + \\ & (k_{11} \sin^2 \theta + k_{22} \cos^2 \theta) \frac{1}{r^2} \frac{\partial^2 T}{\partial \phi^2} + \\ & k_{22} \frac{\partial^2 T}{\partial z^2} + 2(k_{22} - k_{11}) \sin \theta \cos \theta \frac{1}{r} \frac{\partial^2 T}{\partial \phi \partial r} = 0 \end{aligned} \quad (6)$$

Also, the flux equation can be written as:

$$\begin{aligned} q_r &= -(k_{11} \cos^2 \theta + k_{22} \sin^2 \theta) \frac{\partial T}{\partial r} - (k_{22} - k_{11}) \sin \theta \cos \theta \frac{1}{r} \frac{\partial T}{\partial \phi} \\ q_\phi &= -(k_{22} - k_{11}) \sin \theta \cos \theta \frac{\partial T}{\partial r} - (k_{11} \sin^2 \theta + k_{22} \cos^2 \theta) \frac{1}{r} \frac{\partial T}{\partial \phi} \end{aligned} \quad (7)$$

$$q_z = -k_{22} \frac{\partial T}{\partial z}$$

NUMERICAL SOLUTION METHOD

Due to complexity of the above mentioned equations, some numerical solution methods is necessary. The finite difference method (FDM) and in this case FTCS (Forward in time and central in space) was selected for solving the problem.

In Fig. 1, used schematic meshing for the cylindrical vessel is represented with inner radius, a and outer radius, b , in polar coordinate (r, ϕ) .

Temperature in an arbitrary point in the cylinder is the function of the coordinates of that point. i.e: $T(\phi, r, z) = T(i\Delta r, j\Delta \phi, k\Delta z) \equiv T_{i,j,k}$

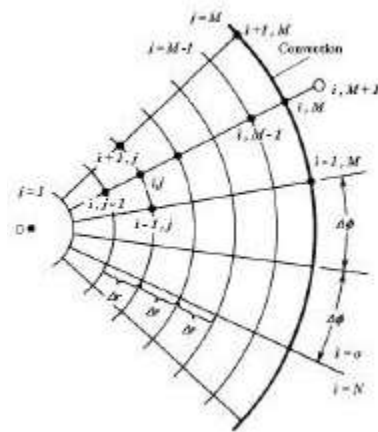


Fig. 1: Two dimensional schematic of meshing in a cylindrical coordinates and virtual node $i, M+1$

$$\begin{aligned} i &= 0, 1, 2, \dots, N \\ j &= 0, 1, 2, \dots, M \\ k &= 0, 1, 2, \dots, O \end{aligned} \quad (8)$$

And r, ϕ and z are restricted as:

$$\begin{aligned} a &\leq r < b, \\ 0 &\leq \phi \leq 2\pi, \\ 0 &\leq z \leq h \end{aligned} \quad (9)$$

Suppose in the $r=b$, the heat transfer to be through the convection. Thus we have:

$$k \frac{\partial T}{\partial r} + hT = hT_\infty \quad (10)$$

DISCRETIZATION METHOD

We can adjusting the equation (6) in the following form:

$$\begin{aligned} & (k_{11} \cos^2 \theta + k_{22} \sin^2 \theta) \left[\frac{1}{r} \frac{\partial T}{\partial r} + \left(\frac{\partial^2 T}{\partial r^2} \right) \right] + \\ & (k_{11} \sin^2 \theta + k_{22} \cos^2 \theta) \frac{1}{r^2} \frac{\partial^2 T}{\partial \phi^2} + \\ & k_{22} \frac{\partial^2 T}{\partial z^2} + 2(k_{22} - k_{11}) \sin \theta \cos \theta \frac{1}{r} \frac{\partial^2 T}{\partial \phi \partial r} = \\ & \rho C_p \frac{\partial T(r, \phi, z, t)}{\partial t} \end{aligned} \quad (11)$$

Because this problem is not time dependent, variation of T related to time in right side of equation(11) is zero. This adjusting is necessary for using equation (6) in FTCS method. The two sides of

equations (11) can be divided by ρC_p and we define the below constants for each lamina:

$$a = \frac{k_{11} \cos^2 \theta + k_{22} \sin^2 \theta}{\rho C_p}, \quad b = \frac{k_{11} \sin^2 \theta + k_{22} \cos^2 \theta}{\rho C_p}$$

$$c = \frac{k_{22}}{\rho C_p}, \quad d = \frac{2(k_{22} - k_{11}) \sin \theta \cos \theta}{\rho C_p} \quad (12)$$

Now the discretized form of energy equation can be written as:

$$\frac{T_{i,j,k}^{n+1} - T_{i,j,k}^n}{\Delta t} =$$

$$a \left(\frac{T_{i,j+2,k}^n - 2T_{i,j,k}^n + T_{i,j-2,k}^n}{\Delta r^2} \right) + \frac{a}{r_j} \left(\frac{T_{i,j+1,k}^n - T_{i,j-1,k}^n}{\Delta r} \right) +$$

$$\frac{b}{r_j^2} \left(\frac{T_{i+2,j,k}^n - 2T_{i,j,k}^n + T_{i-2,j,k}^n}{\Delta \phi^2} \right) + \quad (13)$$

$$c \left(\frac{T_{i,j,k+2}^n - 2T_{i,j,k}^n + T_{i,j,k-2}^n}{\Delta z^2} \right) +$$

$$\frac{d}{r_j} \left(\frac{T_{i+1,j+1,k}^n - T_{i-1,j+1,k}^n - T_{i-1,j-1,k}^n + T_{i+1,j-1,k}^n}{4\Delta \phi \Delta z} \right)$$

At this stage, for the first series operations, i.e. $T_{i,j,k}^0$ an arbitrary temperature for internal nodes and for the boundary nodes the boundary conditions must be assumed.

BOUNDARY CONDITIONS

As it was said before, the boundary conditions for the radial orientation includes two requirements; heat transfer on outer boundary. Since the heat transfer coefficient is unknown (can not be prescribed), it may be assumed to be proportional to the differences between the boundaries and ambient temperature, i.e:

$$q_r = h(T - T_\infty) \quad (14)$$

where temperature is assumed to be constant in the vessel.

This assumption is correct, because we use laminated cylinder with only constant internal pressure and there is not heating source and so on and we suppose the gas is in the stable condition.

According to Fig. 1, since temperature in the ϕ orientation has an alternately 2π , an accurate boundary condition can be found at that point, that is:

$$T_{0,j,k} = T_{N,j,k} \quad (15)$$

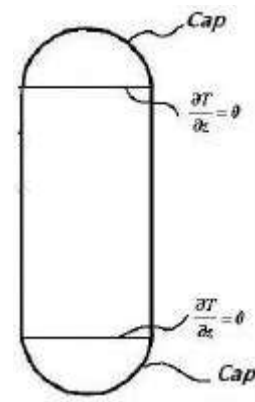


Fig. 2: A schematic of vessel with it's isolated caps

And because there are two caps at the ends of the vessel which includes a small part of total area of vessel, let us assume that there is no heat transfer at the ends, in the other word, we suppose that the caps are isolation.

At last in order to solve the problem for middle layers, we need six boundary conditions for each layer (two boundary conditions for each orientation of r, ϕ, z).

Let us assume that for every arbitrary orientation, for n th middle layer, the temperature and flux on the internal boundary of n th layer equal to these on the external boundary of $(n-1)$ th layer and also, temperature and flux on the external boundary of n th layer is equal to those on the internal boundary of $(n+1)$ th layer. It may be thought that these boundary conditions are more than needed, but they are imperfect. Temperature and flux values are unknowns on the internal layers. By considering every two imperfect conditions together a perfect condition will be formed. It should be noted that, flux values can be obtained via simultaneous solving of equation(7).

PROBLEM DEFINITION

The inner radius and the length of cylindrical section are 151mm and 600mm, respectively. This pressure vessel is fabricated by intersecting filament winding at all sections and hoop filament winding at cylindrical section.

Totally there are eight layers by intersecting filament winding and two layers with hoop filament winding. Three major and convectional stacking sequences that are important due to mechanical design are studied here. The twist angle of fiber, θ , is measured due to cylinder axis. These angles are shown in Table 1.

For all the stacking sequences, the layer thicknesses are 2.193mm, except the-88 and 88 that are

Table 1: Three stacking sequence A, B and C

Layer's No.	Stacking sequence A	Stacking sequence B	Stacking sequence C
1	25.4	25.4	-88.0
2	29.6	-25.4	-53.8
3	53.7	29.6	-53.7
4	53.8	-29.6	-29.6
5	88.0	53.7	-25.4
6	-88.0	-53.7	25.4
7	-53.8	53.8	29.6
8	-53.7	-53.8	53.7
9	-29.6	88.0	53.8
10	-25.4	-88.0	88.0

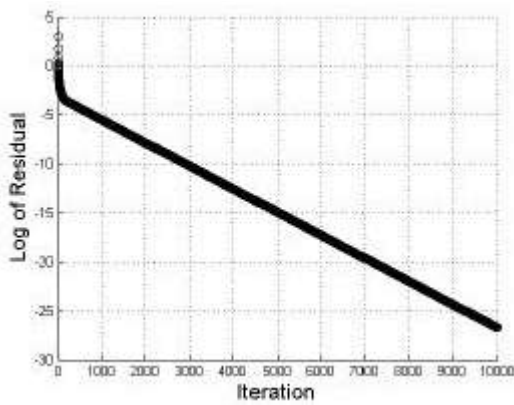


Fig. 3: Log of residual in terms of number of response iterations

2.02 mm. These results are related to carbon epoxy composite T300/5208. The uniform internal temperature of vessel is 350°k and ambient temperature is 297°k. This temperature difference is intended for obtaining more clear results and it may only occur under special condition.

Boundary condition on outer surface of vessel is supposed as convection. Heat transfer coefficient is one of the major parameters in convection. Herein the effects of these parameters on heat distribution are checked via using values shown in Table 2. In this paper, for all temperature distributions, convection coefficient is obtained equal to 21 w/m².°C.

In this problem, convergence is depend on mesh size, forward time steps, initial guess, longitudinal and transverse conductivity coefficient values, heat conduction coefficient value and etc. In Fig. 3, you can see an example of Log of residual or errors variations in terms of the number of response iterations in this section.

TEMPERATURE DISTRIBUTIONS IN DIFFERENT LAYERS

The Temperature distributions in the layers are shown in Fig. 4-6 according to number of nodes in the each layer. Due to small thickness of layers, the number of nodes is a few. In Fig. 7, the temperature distribution for each layer for stacking sequence of C is represented too.

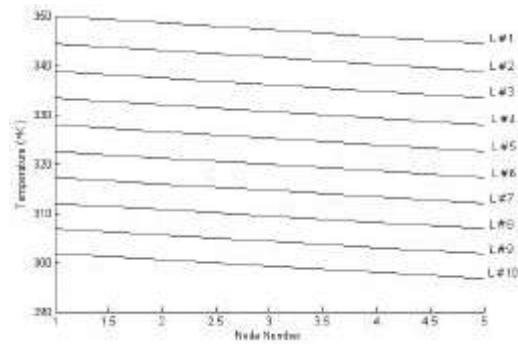


Fig. 4: Temperature distribution in nodes of each layer for stacking sequence of A

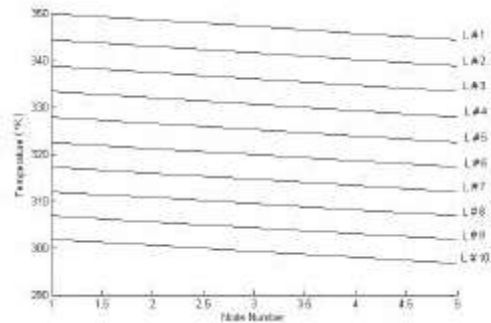


Fig. 5: Temperature distribution in nodes of each layer for stacking sequence of B

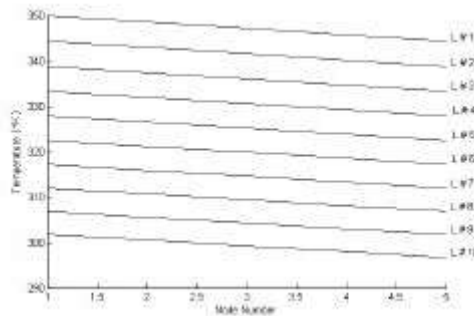


Fig. 6: Temperature distribution in nodes of each layer for stacking sequence of C

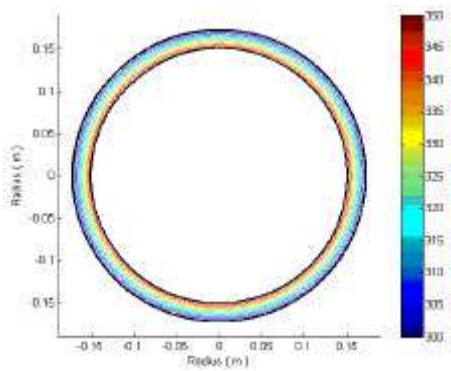


Fig. 7: Temperature distribution contour in nodes of each layer for stacking sequence of C

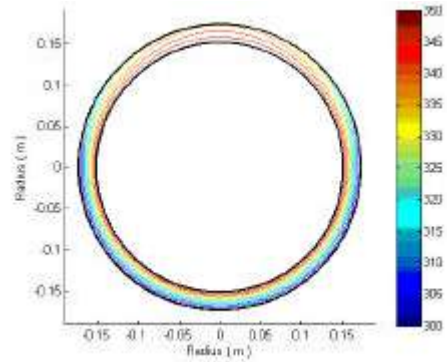


Fig. 11: Temperature distribution as contour in nodes of each layer for stacking sequence of C

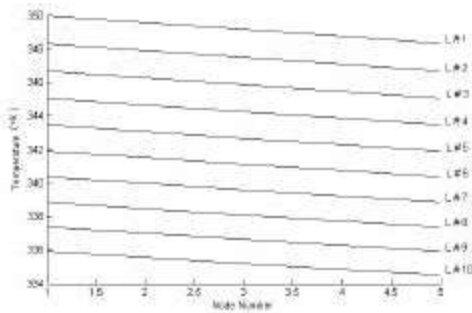


Fig. 8: Temperature distribution in nodes of each layer for stacking sequence of A

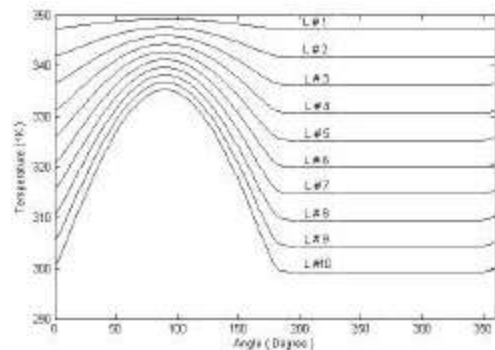


Fig. 12: Temperature distribution behavior in vessel's layers for stacking sequence of A exposed to radiation

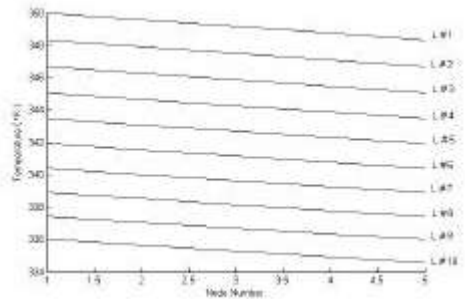


Fig. 9: Temperature distribution in nodes of each layer for stacking sequence of B

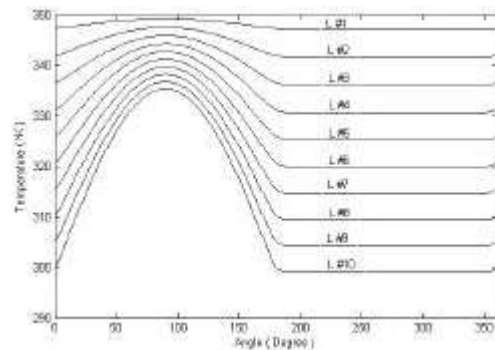


Fig. 13: Temperature distribution behavior in vessel's layers for stacking sequence of B exposed to radiation

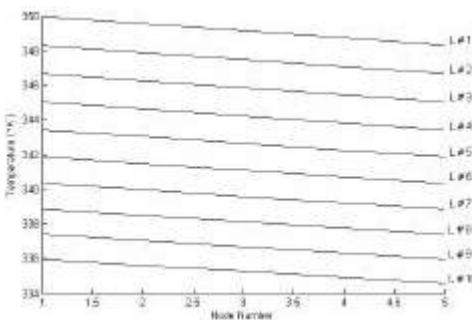


Fig. 10: Temperature distribution in nodes of each layer for stacking sequence of C

If we assume that this vessel is exposed to a 500 watt radial radiation source that placed in a far distance, a new boundary condition will be added. In this configuration we see that the change of temperature behavior in more than the half of the vessel that exposed to the radiation source. It is clear that there is temperature magnitude at location that radiation

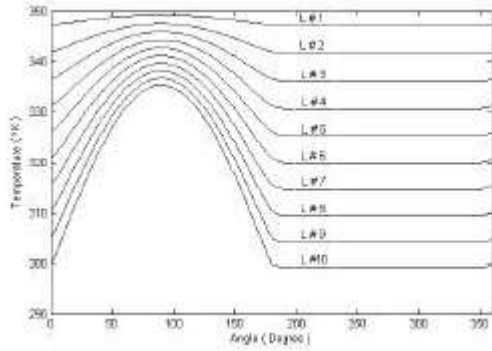


Fig. 14: Temperature distribution behavior in vessel's layers for stacking sequence of C exposed to radiation

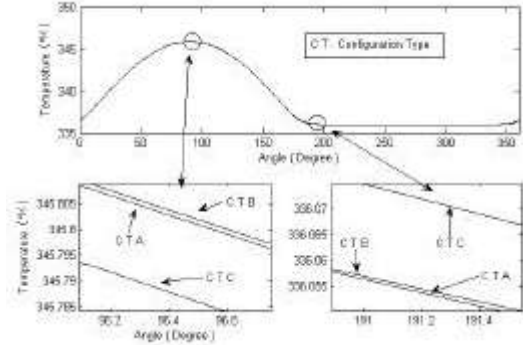


Fig. 17: Temperature distribution changes in 3th vessels' layer in radiation condition

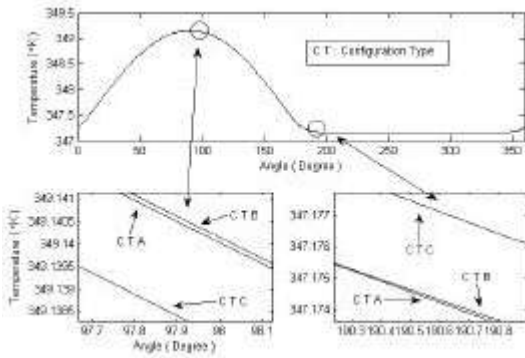


Fig. 15: Temperature distribution changes in 1th vessel's layer in radiation condition

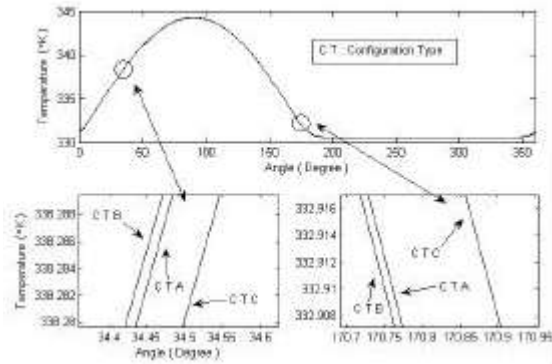


Fig. 18: Temperature distribution changes in 4th vessels' layer in radiation condition

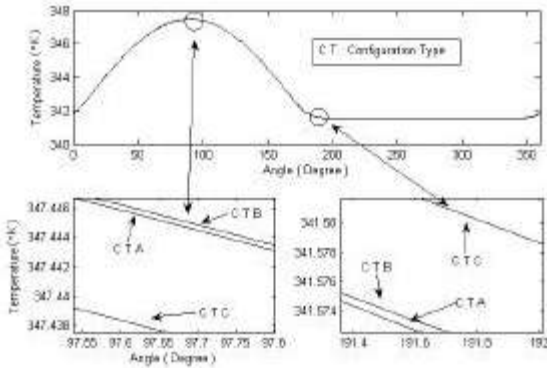


Fig. 16: Temperature distribution changes in 2th vessels' layer in radiation condition

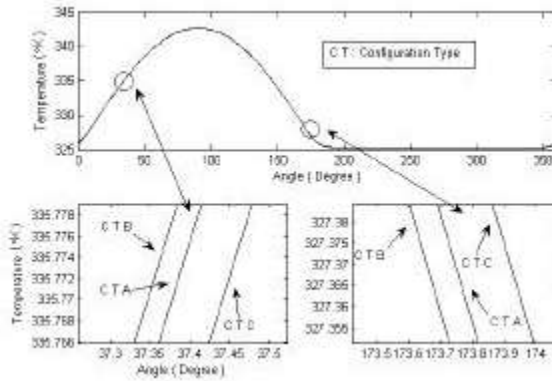


Fig. 19: Temperature distribution changes in 5th vessels' layer in radiation condition

orientation and normal vector of surface have same direction. In Fig. 8-10. You can see the effect of this new condition with contour in Fig. 11.

Based on the radiation, the temperature distribution behavior in the inner nodes of each layer with the tangential direction for the stacking sequences of A, B and C are shown in Fig. 12-14. As you can see, the

radiation changes the temperature uniformity in about 190° up to 350° and cause the relatively thermal shock in-10° to 190°. According to our prediction, the maximum value is occurred in 90° and external layers show the high temperature changes. An important note is that, various stacking sequences cause no effect on temperature distribution and there is a full compatibility

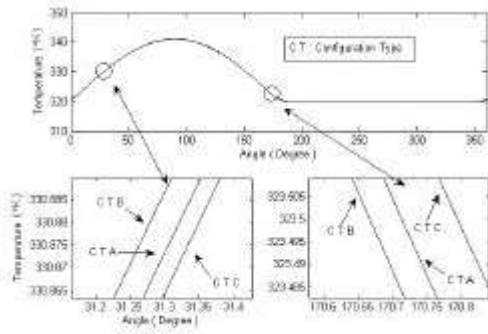


Fig. 20: Temperature distribution changes in 6th vessels' layer in radiation condition

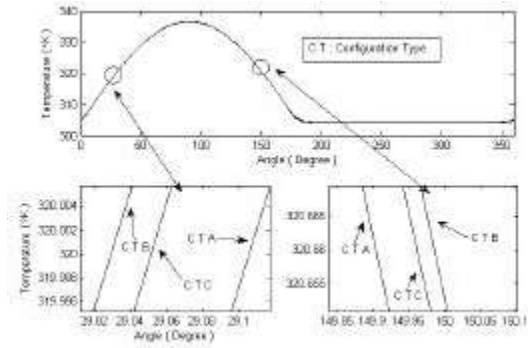


Fig. 23: Temperature distribution changes in 9th vessels' layer in radiation condition

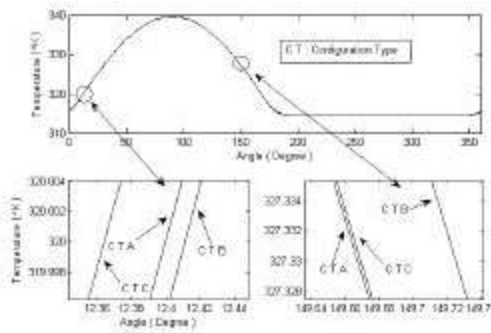


Fig. 21: Temperature distribution changes in 7th vessels' layer in radiation condition

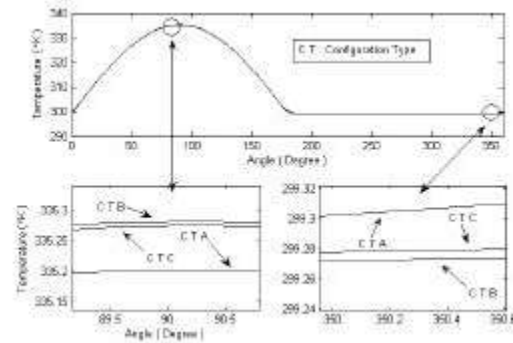


Fig. 24: Temperature distribution changes in 10th vessels' layer in radiation condition

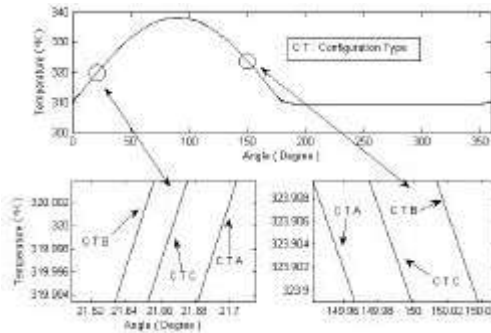


Fig. 22: Temperature distribution changes in 8th vessels' layer in radiation condition

between profiles of temperature distributions for three stacking sequences.

In order to get the final result, the temperature distribution diagrams for each layer of three stacking sequences are provided and a random point is enlarged. This results are shown in Fig. 15-24.

RESULTS AND CONCLUSION

Using a laminated vessel with optimum stacking sequence is the most important portion in designing a

composite structure and it is important that we know stacking sequence affect on the other engineering parameters. For example, heat transfer and temperature distribution in structure layers, are considered among these parameters. Figures 3-14 does not show a large changes from the effect of stacking sequence on temperature distribution at each layer. In all figures, it was found that different stacking sequences have negligible difference and don't follow a certain procedure. So it is not possible to answer the question which stacking sequence has the higher temperature distribution profile at about 80° to 100°.

Generally, we can conclude that stacking sequence has no significant effect on the temperature distribution.

REFERENCES

1. Bulavin, P.E. and V.M. Kashcheev, 1965. Solution of the nonhomogeneous heat conduction equation for multilayered bodies. International Chemical Engineering, 5: 112-115.
2. Mulholland, G.P. and M.H. Cobble, 1972. Diffusion through composite media. Journal of Heat and Mass Transactions, 15: 147-160.

3. Han, L.S. and A.A. Cosner, 1981. Effective thermal conductivities of fibrous composites. *ASME Journal of Heat Transactions*, 103: 387-392.
4. Azcvedo, J.P.S. and L.C. Wrobel, 1988. Non-linear heat conduction in composite bodies: A boundary element formulation. *International Journal of Numeric Methods and Engineering*, 26: 19-38.
5. Chen, F., J. Gill, D. Harmon, T. Sullivan, A. Strong, B. Li, H. Rathore and D. Edelstein, 2006. Determination of the thermal conductivity of composite low-k dielectrics for advanced interconnect structures. *Microelectronics Reliability*, 46: 232-243
6. Archer, R. and R.N. Horne, 1998. Flow simulation in heterogeneous reservoirs using dual reciprocity boundary element method and the Green element method. *ECMOR*, 6: 13.
7. Okey Oseloka Onyejekwe, 2002. Heat conduction in composite media: A boundary integral approach. *Computers and Chemical Engineering*, 26: 1621-1632.
8. Miller, J.R. and P.M. Weaver, 2003. Temperature profiles in composite plates subject to time-dependent complex boundary conditions. *Composite Structures*, 59: 267-278.
9. Tittle, W.C. and V.L. Robinson, 1965. Analytical solution of conduction problems in composite media. ASME paper, 65-WA-HT.
10. DeMonte, F., 2000. Transient heat conduction in one-dimensional composite slab. A 'natural' analytic approach. *Intl. J. Heat. Mass. Trans.*, 43: 3607-3619.
11. Onyejekwe, O.O., 1996. Green element description of mass transfer in reacting systems. *Numerical Heat Transfer Part B*, 30: 483- 498.
12. Heisler, M.P., 1947. Temperature charts for induction and constant temperature Heating. *Trans. ASME*, 69: 227-236.
13. Ozisik, M.N., 1968. Boundary value problems of heat conduction. Scranton, PA, International Textbook, 1968.
14. Onsagar, L., 1931. *Phys. Ref.*37", 38: 405-426.
15. Carslaw, H.S. and J.C. Jaeger, 1959. *Conduction of Heat in Solids*. Oxford University Press.
16. Alderson, K.L., 1992. Failure Mechanics during the Transverse Loading of Filament-woun pipes under static Low Velocity impact condition. *Composite*, 23: 167-173.